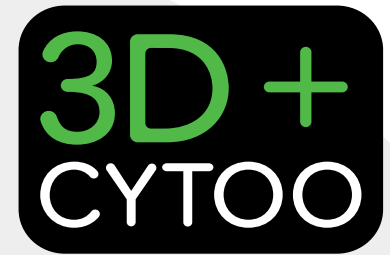


Micropatterns for 3D+ epithelial cell culture: new high content screening opportunities for cancer and disease research*



Applications using acini and the 3D morphogenesis assay

Assay relevance is key to both phenotypic and targeted screening. For this reason, the pharmaceutical industry is increasingly turning towards the use of more physiological cell models. For decades, specialist academic labs have been using 3D cell cultures to grow acini* (See Glossary), the basic structural unit of organs such as the kidney, lung, breast, pancreas, oviduct, respiratory tract, salivary glands, prostate and intestine. Acini are used as *in vitro* models of normal epithelial glandular tissue to study factors involved in early carcinoma development¹, the epithelial-mesenchymal transition², drug resistance³, cilia dysfunction related to mutations implicated in ciliopathies⁴ and diseases associated with alterations in apical polarity such as cystic fibrosis, Liddle's syndrome, nephrogenic diabetes insipidus, Dubin-Johnson syndrome and polycystic kidney disease⁵. In addition, infectious virus and bacteria such as adenovirus, reovirus, hepatitis C virus and *Helicobacter pylori*, depend on polarized epithelia for their transmission. Human organotypic cultures are also being used to discover clinically relevant biomarkers and assess the effect of exposure to environmental agents during development⁶. Indeed, due to their clonal morphogenesis in a surrounding ECM matrix, acini are more physiologically relevant and thus closer to the *in vivo* situation than multicellular aggregates (or spheroids) formed in suspension and in the absence of adhesive substrates. Despite being powerful tools, acini are rarely exploited by industrial laboratories for drug discovery and pharmacological screening, primarily due to the lack of robust epithelial models and the very specific protocols that are expensive to optimize, technically demanding and inappropriate for automation routines.

In this Application Note, CYTOO responds to the need for a miniaturized mesoscale 3D cell culture test platform enabling routine formation of acini. Using micropattern arrays and MDCK kidney cells, we demonstrate optimization of the acini platform and compare our results in parallel with MDCK acini formed on non-micropatterned surfaces. We provide two examples of different approaches that can be used for further assay development and are possible exclusively on micropatterns. The first example demonstrates polarization of 3 and 6 day old acini while the second example shows early lumen formation in polarized 2-cell stage acini. We conclude by confirming acini formation on micropatterns with other cell models.

Reproducible	1) Efficient production of acini grown in organotypic cultures in chip or 96-well SBS formats 2) Growth of acini with homogenous size and morphology for robust statistical analyses 3) No aggregation of 3D structures during growth, simplifying image segmentation 4) Single cell seeding on micropatterns to ensure clonal growth
Fast and easy	5) Standardized protocols for specific models accelerating routine adoption of 3D culture and de-risking assay development 6) Difficult gel coating step is replaced with a range of surface protein coatings eg. laminin, collagen, fibronectin 7) No loss of acini during pipetting procedures such as immunostaining or addition of compounds 8) Acini grow in a single plane and closer to the glass surface reducing issues with microscope focusing, speeding up image acquisition and facilitating high resolution and live cell microscopy
Flexible	9) Supports long-term (over 3 weeks) development of acini 10) Demonstration with a range of complex epithelial cell models eg. MDCK, Caco-2, NMuMG, RWPE-1, LLC-PK1

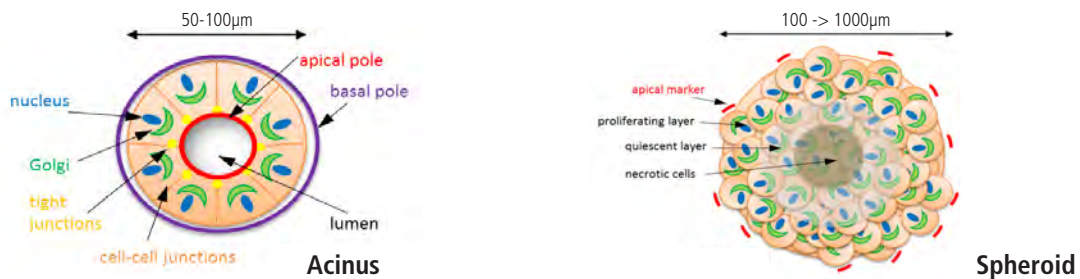
Table 1: Ten key advantages of 2D+ micropatterns for 3D cell culture

* CYTOO Cell Architects, 7 parvis Louis Néel, Grenoble, France www.cytoo.com

Glossary

Acini ~ Functional glandular structures consisting of a single layer of polarized epithelial cells that surround a central liquid-filled lumen. Also referred to as cysts or follicles, acini are growth arrested hollow spheres with diameters around 50-100 μm . Acini are important *in vitro* models of healthy tissue not to be confused with **spheroids that represent pre-vascular phase solid tumors and which are compact cell aggregates without lumen growing to diameters up to 1000 μm or more**. Also, unlike spheroids, acini form clonally following a specific morphogenesis developmental program.

Only certain phenotypically normal non-transformed epithelial cell lines have the capacity to establish polarized structures with apicobasal membrane polarity and an apical pole. A few cancer-derived epithelial cell lines (eg. colon cancer-derived Caco-2, prostate cell lines DU145 and PC-3) can develop into organized structures with a hollow lumen, similar to the acini formed by healthy epithelial cells. However, they are metastable and tend to develop internal cell masses over time or produce a mixed population of acini and spheroids due to compromised basement membrane assembly and apical pole establishment^{7,8}. Tumor cell lines, in particular those expanded from non-carcinoma tumors can form only spheroids in 3D culture.



Limits of currently used methods for growing 3D acini

In order to undergo differentiation and cystogenesis to form acini, epithelial cells must be exposed to a 3D extracellular matrix (ECM) environment. Depending on the cell type, acini are traditionally grown in purified collagen-I hydrogels or Matrigel®, a laminin-rich commercially available basement membrane extract isolated from mouse tumor tissue. Two set-ups exist for doing 3D culture: individual cells are completely mixed with the gel (known as the fully embedded method) or seeded at the interface between two gel layers of different concentrations (known as the sandwich or overlay method). Both methods impose significant problems for the 96-well format (Table 2).

Fully embedded	Sandwich or overlay
<p>Cells are seeded throughout the gel so acini form across several Z planes. Cells are distributed randomly within the gel resulting in acini that overlap or fuse into one another and grow at different rates giving a population that is heterogeneous in size and complicated to segment by automatic image analysis. Antibody penetration is impaired by the thick gel coating so acini have to be cryosectioned</p>	<p>Due to high surface tension of hydrogels, a meniscus is formed in small wells inducing cells to collect in the middle of the well. The less flat the plane of the gel, the more the acini will be in different planes of focus leading to increased acquisition time and microscope focusing problems during high content imaging. Bubbles can form allowing cells to come into contact with the culture surface where they start to spread as a 2D monolayer.</p>
<p>High cost per well ratio Immunostaining analysis is complicated by high non-specific background signals due to the gel Concentrated viscous hydrogels are tricky to prepare, manipulate and difficult to pipette in low volumes</p>	

Table 2: limits of current 3D methods

Below we show how we addressed each of these issues to improve the 3D acini system.

Cell source considerations

Only a restricted number of immortalized epithelial cell lines actually have the capacity to form acini in 3D culture. Even cell lines with the same origin show strong inconsistencies in their differentiation capabilities. There are more than 9 unique MDCK strains available for purchase through the ATCC and ECACC. We tested three MDCK variants for their potential to form acini in conventional 3D culture conditions. After 3 days growth in Matrigel, MDCK NBL-2 (ATCC cat No. CCL-34) and MDCKII (ECACC cat No. 00062107) formed acini (Fig. 1A, C) while variant MDCK.1 (ATCC cat No. CRL-2935) formed a monolayer only (Fig. 1B). Since MDCK NBL-2 exhibited obvious heterogeneity in 2D culture, we proceeded to optimize conditions for acini formation on micropatterns using MDCKII.

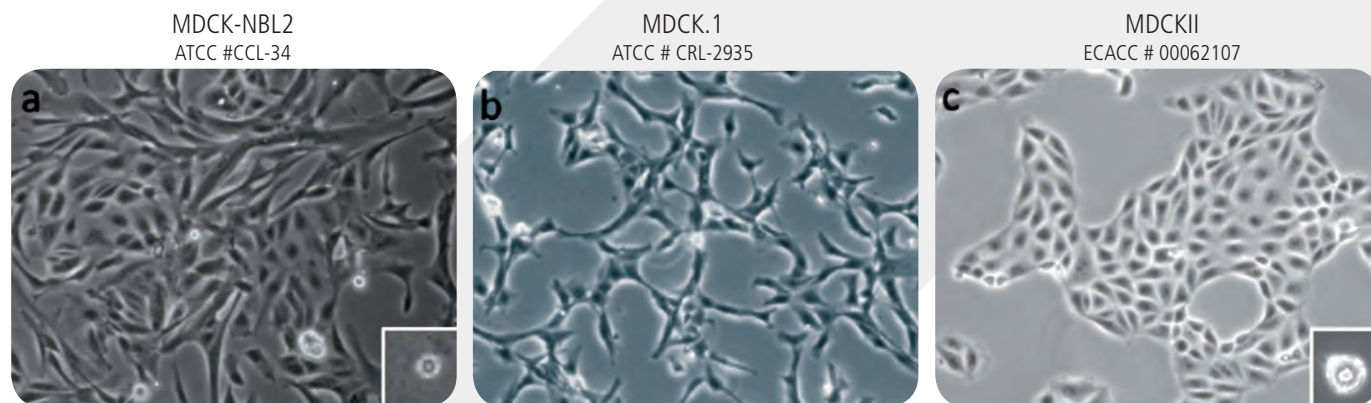


Figure 1 (A-C). Phase images of MDCK variants in 2D culture on plastic. Insets show details of acini morphology and size obtained for each variant after 3 days in 3D culture conditions. Only the variants MDCK-NBL2 (A) and MDCKII (C) formed acini with hollow lumens.

Evaluation of MDCKII acini formation on 2D and 2D+ rigid surfaces

The fully embedded and overlay methods of 3D culture rely on seeding cells in or on a soft hydrogel that has a mechanical compliance of <0.5 kPa, resembling that of the native tissue⁹ (Fig. 2A). In order to replace the cumbersome procedures associated with coating concentrated viscoelastic gels for 3D culture, we tested if MDCKII polarization and lumen formation can take place on rigid glass surfaces that are either planar (termed 2D) or micropatterned (termed 2D+). Laminin-111 (formerly known as laminin-1) at 20 $\mu\text{g}/\text{ml}$ was used to coat the glass surface since it is the chief component of Matrigel and the basal presence of laminin-111 added exogenously or synthesized *de novo* is essential for orientating cell polarity¹⁰. For all experiments, cells were grown in complete medium supplemented with 2% Matrigel because an ECM overlay is necessary for initializing interactions on the dorsal surface of cells in order to form the third dimension. This low Matrigel concentration is compatible with automated high throughput systems.

MDCKII cells were thus seeded on laminin-111 coated glass coverslips (2D) or on CYTOOchips (2D+) with micropatterned disk sizes of 1600, 1100 and 700 μm^2 . After 3 days of growth, the samples were fixed and immunostained with a monoclonal antibody against the apical domain marker gp135/podocalyxin¹¹, phalloidin as a probe for F-actin and Hoechst 33342 for fluorescent staining of nuclei. Throughout this Application Note, we used the non-confocal Cellomics CellInsight system and integrated software to automatically image, identify and score acini using an unbiased approach at 10x magnification (as described in Point 10. Data Analysis). **The CellInsight was efficient in automatically detecting and identifying acini on 2D and 2D+ surfaces due to the fact that the acini are present in one focal plane.** This is not the case for acini formed in or on gel substrates where due to variations in the thickness of gel one is dependent on a confocal system and multiple Z sections in order to capture enough in-focus samples, especially at higher magnifications. Acini were defined as the number of structures possessing gp135 and cortical F-actin concentrated at a central lumen (Fig. 2B).

The results (Fig. 3B) indicated that in the presence of 2% Matrigel supplemented medium, **MDCKII cells can form >70% properly polarized acini after 3 days culture on both non-patterned and micropatterned rigid glass surfaces without a gel undercoating.** This high percentage is equivalent to that reported by others using this cell type under standard 3D culture methods. The other 10-30% of structures had an abnormal cellular organization and failed to form a central lumen with the apical marker gp135 being retained at the basal membrane (Fig. 2B). Thus, **full or partial exposure of MDCKII cells to a soft gel matrix is not essential for acini morphogenesis allowing us to establish a simplified system for 3D culture** on protein coated glass that is more advantageous for high throughput screening and imaging.

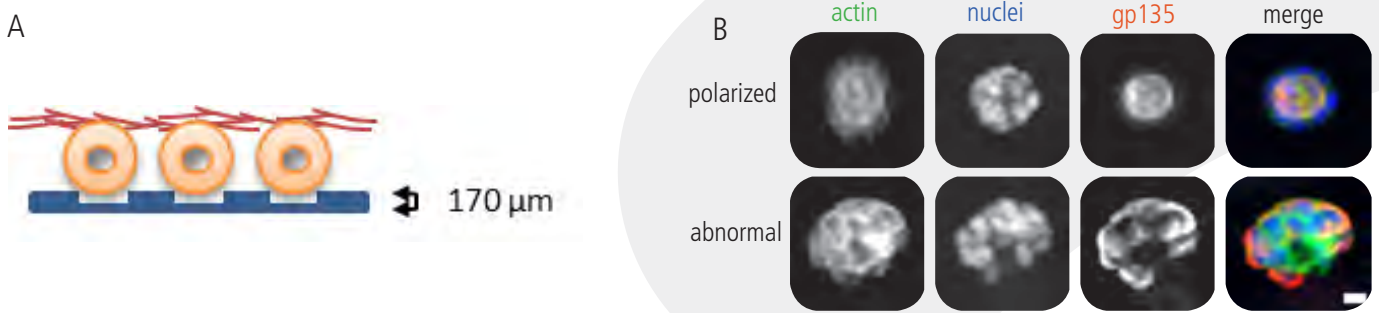


Figure 2 (A). Experimental set up for 3D cell culture on CYTOO micropatterns. Single cells are seeded on protein coated micropatterns on thin glass of 170 μm thickness only (in blue). Cells are overlaid with medium containing serum and low concentrations of Matrigel (in red). On micropatterns, acini develop in a single focal plane. (B) Correct localization of the apical marker gp135 and concentration of cortical F-actin at the lumen was used to qualify the existence of polarized acinar structures. Scale bar: 10 μm .

Optimization of acini formation on 2D+ micropatterns

In the presence of laminin-111 coating, MDCKII cells underwent acini morphogenesis equally efficiently on 2D surfaces as on all three micropattern disk sizes: 1600, 1100 and 700 μm^2 (Fig. 3A). Analysis of the size of MDCKII acini with a normal lumen on non-patterned and micropatterned disks indicated that the 700 μm^2 disk ($\phi = 30 \mu\text{m}$) promotes the formation of a population of acini that are statistically significantly smaller ($752 \pm 264 \mu\text{m}^2$) than those formed on non-patterned surfaces ($912 \pm 322 \mu\text{m}^2$) or on 1600 or 1100 μm^2 disks suggesting that the 700 μm^2 disk can confine the acini without affecting polarization and lumen efficiency (Fig. 3B). However, the overall acini population on 700 μm^2 disks was not more homogenous and the range of acini sizes was equivalent for both non-patterned and 700 μm^2 disks as indicated by the coefficient of variation (CV) of acini area (CV=34%). Because in laminin-rich microenvironments MDCKII cells rapidly round up undergoing polarization and lumen formation straightaway, the laminin-111 coated fully adhesive micropatterns have little influence on acini formation which proceeds as described for traditional 3D culture.

The efficiency of lumen formation was also tested using other micropattern shapes including H-shape known to stabilize epithelial junctions in cell doublets¹² and Y-shape where the Y intersection and arms inscribe a circle. For both geometries the efficiency of acini formation was invariably lower (60%) than the disk shape (Fig. 3A and B). This indicates that non-fully adhesive micropattern shapes can have a certain (negative) influence on early events during lumenogenesis (eg. perhaps polarization, membrane separation or spindle orientation during cell division). **For this reason, we concluded that disks are to be favored for acini formation and we used the 700 μm^2 disk for all subsequent experiments.**

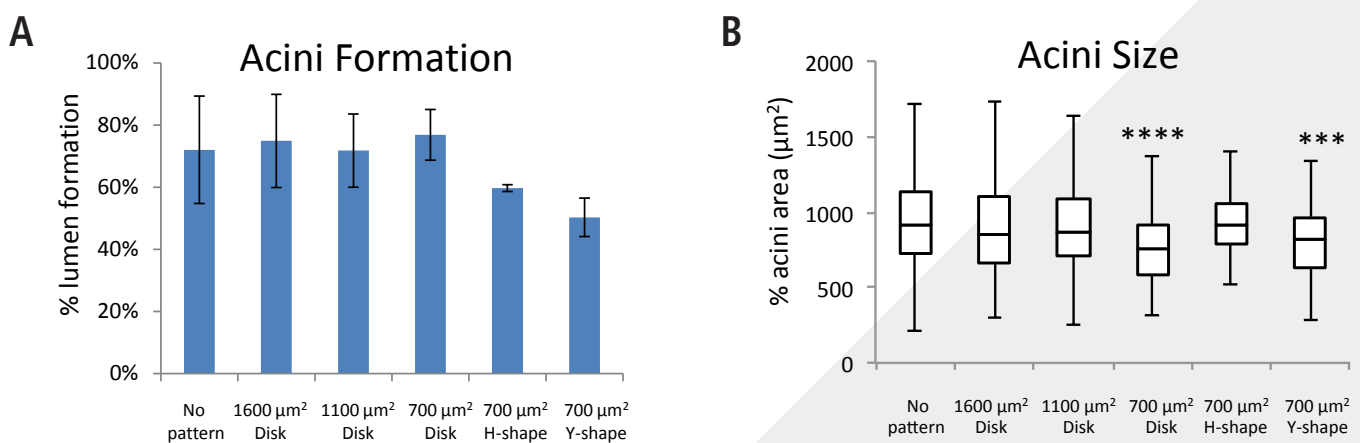


Figure 3 (A) MDCK cells were cultured on non-patterned laminin coated surface or on laminin coated disks of different surface areas. After 72 hrs, samples were fixed and stained and quantified for the presence of polarized lumens. Results represent the mean \pm SD from two independent experiments. (B) Graph of polarized acini size for the same two experiments shown in A. Median values are shown by the horizontal bar within each box; boxes show 25th and 75th percentiles; whiskers show the spread of the data. $n = 100-650$ structures analyzed for each sample. P -values < 0.001 vs. non-patterned control group are signified by (***) and < 0.0001 by (****).

📌 The limits of 2D and the advantages of 2D+: micropatterns prove essential for long-term 3D organization

We have shown above that acini formation on laminin-111 coated micropatterns (2D+) is comparable in rate and efficiency to that on laminin-111 coated glass substrates (2D) and consistent with growth in normal 3D Matrigel culture conditions¹³ reaching >70% over 3 days. After 6 days in 3D culture however, a substantial degeneration of the acini occurred in the absence of micropatterns including a deformation of shape, a greater variation in structure sizes and the appearance of multiple lumens (Fig. 4A). Overall levels of polarized acini decreased from 90% to 48% with a concomitant increase in cell spreading to flat monolayers (Fig. 4C). On the contrary, at 6 days on 700 μm^2 disk micropatterns, acini continued to expand and increase in size (median 1682 μm^2 at 6 days), the majority of cyst cross-sections appeared circular with a single lumen and polarized acini levels remained at 90% (Fig. 4B and C). This suggests that a laminin-111 coated 2D surface alone is insufficient for supporting long-term 3D epithelial acinar organization and **in the absence of an underlying soft substratum gel layer, laminin-111 coated micropatterns (2D+ surfaces) can provide the necessary geometrical and physical confinement to compensate and sustain long-term 3D cell culture.**

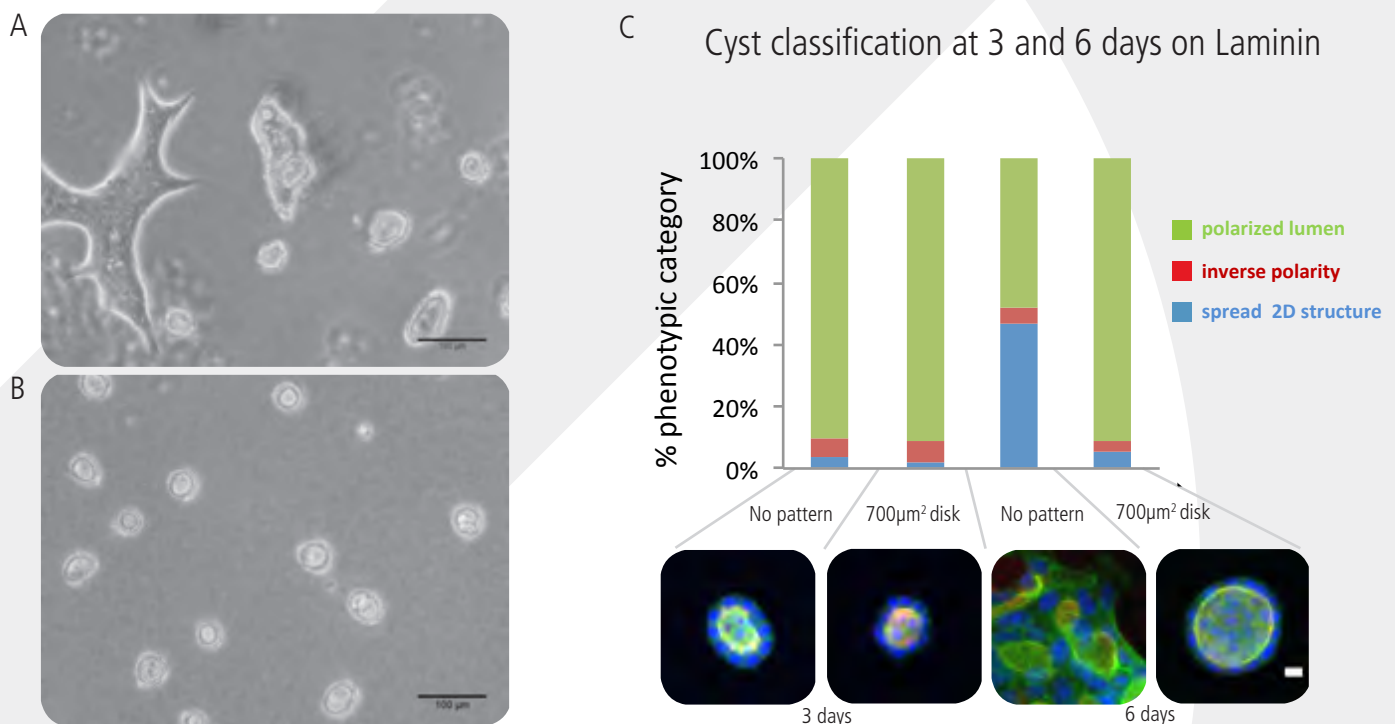


Figure 4. MDCK acini formation at 6 days after seeding on laminin-111 coated (A) glass coverslips or (B) 700 μm^2 disk micropatterns. Without micropatterns, acini are less circular, often with multiple lumens and start to spread as a polarized monolayer. In contrast, when cultured on micropatterns acini are homogenous in size and shape with a well developed lumen and continue to grow as an array. Scale bar: 100 μm . (C) Quantification at 3 and 6 days on laminin-111 coating after fixing and staining. Based on localization of the apical marker, structures were phenotypically classified into one of three categories: acini with apically polarized gp135 (green), abnormal cysts with mistargeted basal location of gp135 referred to as inverse polarity (red) and structures that proliferate as a polarized monolayer (blue). Below are shown composite images of the most typical structures present for each experimental condition. Actin green, gp135 red, nuclei blue. Scale bar: 10 μm .

📌 Acini formation on other ECM coatings is only possible with micropatterns

We tested the ability of MDCKII cells to form acini on non-micropatterned and micropatterned surfaces coated with other commonly used ECM proteins, namely collagen-I and fibronectin at 20 $\mu\text{g}/\text{ml}$. Unlike laminin-111, an intrinsic component of basement membranes deposited beneath epithelia, collagen-I and fibronectin are part of the stroma/interstitial matrix that impart structural support.

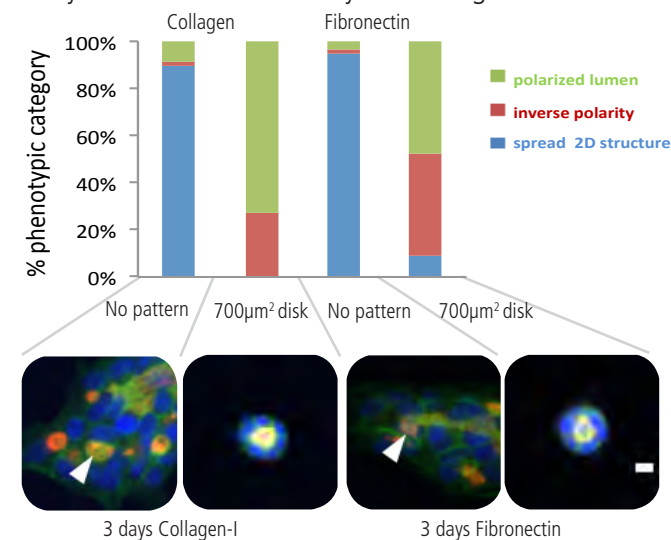
On 700 μm^2 collagen-I coated disks, the percentage of acini at 3 days was 70% (Fig. 5A), almost as efficient as on laminin-111 ECM. Analysis of the acini area showed that acini were typically slightly smaller in size than those grown on laminin-111 coated 700 μm^2 disks (median $557 \pm 85 \mu\text{m}^2$; Fig. 5A). Collagen-I coated 700 μm^2 disks however were much more effective than laminin-111 for obtaining a uniformly-sized population as indicated by the narrower size range distribution and CV value of 15% (Fig. 5B).

The increased influence of collagen-I coated micropatterns is likely due to the polarization kinetics of MDCK cells that are slightly delayed in collagen compared to laminin rich environments¹⁴ because cells initially spread must synthesize their own laminin. **This shows that micropatterns of an optimal surface area combined with certain ECM coatings can enable some control of acini growth rate resulting in a more reproducible uniformly sized acini population.**

On fibronectin-coated 700 μm^2 disks, acini formation reached 50%. This is lower than for collagen-I and laminin-111 coatings and there was a higher proportion of abnormal round structures with “inverted” polarity present (43%; Fig. 5A). The sizes of the acini were equivalent to those formed on laminin-111 coated 700 μm^2 disks with a median area of $748 \mu\text{m}^2 \pm 191$ and a CV of 23% (Fig. 5A).

The above results show that acini formation can take place on a range of standard protein coatings when using micropatterns. Interestingly, on both collagen-I and fibronectin coated 2D non-micropattern surfaces, acini formation was inexistent with cells growing as monolayers only despite the presence of 2% Matrigel in the growth medium (Fig. 5A). Occasionally polarized lumen-like structures were visible within the monolayer (arrowhead in Fig. 5A). Thus, under conditions where polarization is delayed because of an absence or low level of exogenous laminin forcing cells to synthesize laminin de novo in order to engage polarity, normal acini formation becomes absolutely dependent on micropatterns, as shown here on collagen-I and fibronectin coated surfaces.

A Cyst classification at 3 days on Collagen and Fibronectin



B Acini Size on Different ECMs

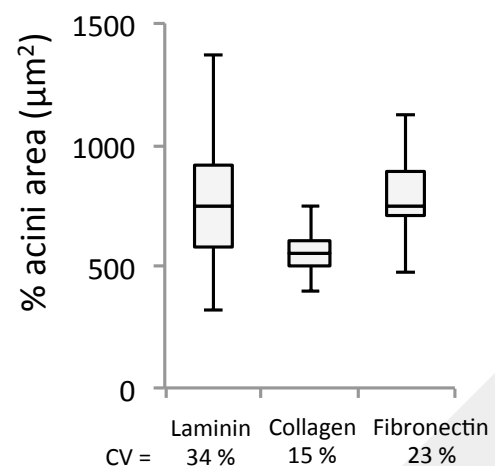


Figure 5. (A) Efficiency of acini formation after 3 days of culture on collagen-I and fibronectin coated 2D and 2D+ surfaces. Structures were fixed, stained and classified as follows: acini with apically polarized gp135 (green), abnormal cysts with mistargeted basal location of gp135 or inverse polarity (red) and structures that proliferate as a monolayer (blue). Composite images of the most typical structures obtained on each protein coating on 2D and 2D+ surfaces are illustrated underneath. Arrowhead indicates lumen like structures that are visible within the cell monolayer. Scale bar: 10 μm . (B) Quantification of acini size and CV values after 3 days of growth on micropatterns coated with different ECM proteins. Median values are shown by the horizontal bar within each box; boxes show 25th and 75th percentiles; whiskers show the spread of the data. The acini population is most homogenous in size on collagen-I coated micropatterns.

📌 Mechanism of lumen formation on micropatterns

Depending on cues from the extracellular microenvironment and the size of cell clusters at initial cell seeding, MDCK cells can form lumens via two different mechanisms¹¹. Within laminin-111 rich Matrigels the dominant process for lumen formation is hollowing driven by polarized membrane trafficking pathways and membrane separation. In collagen gels or the presence of cell aggregates, there exists an apoptotic phase (days 4-10) where up to 35-50% of acini show apoptotic cavitation¹¹. To see which mechanism contributes to cystogenesis on micropatterns, MDCKII cells were cultured on laminin-111 or collagen-I coated disks for 6 days and apoptosis detected by staining with an antibody recognizing activated caspase-3 that is cleaved in apoptotic cells. At 6 days post seeding, on both laminin-111 and collagen-I coated micropatterns, only a low frequency of acini (15-20%) had fragmented nuclei and cleaved caspase-3 positive staining (Fig. 5B). This is close to the 10-15% reported in the literature for traditional Matrigel 3D cultures¹⁰ and suggests that on both laminin and collagen-I coated micropatterns, **MDCKII cells can polarize well and do not rely on apoptosis to form acini with lumens**, following instead the non-apoptotic hollowing process.



Figure 6. Quantification of acini with dying apoptotic cells determined by the presence of cleaved caspase-3 positive nuclei. Cells were fixed at 6 days and stained for gp135, F-actin, cleaved caspase-3 and DNA. Arrowhead indicates fragmented nucleus that is caspase-3 positive. Scale bar: 10 μ m.

📌 Acini growth in 96-well CYTOOplates: pitch is important

To allow drug discovery researchers to perform high content 3D morphogenesis assays, the procedure was optimized to 96-well CYTOOplate format. Using 700 μ m² disks with a pitch of 80 microns, acini formation reached 60% on laminin-111 coated micropatterns and 40% on collagen-I coated micropatterns wells at 3 days. This represents up to 170 acini in a well of a 96-well CYTOOplate (ϕ = 6.3 mm). A low seeding density (1500 cells/well) was preferred in order to encourage clonal growth. An 80 μ m pitch provided sufficient spacing for acini analysis at 3 days (Fig. 7A). At 6 days culture however, acini started to touch and spread into one another due to expansion (Fig. 7B). This illustrates the importance of considering optimal micropattern pitch layout during acini assay development. A small spatial distribution is preferred for providing enough sample replicates for enhanced statistical confidence and maximizing the number of objects per field of view to reduce acquisition times but must be large enough to prevent structures fusing into one another at later time points.

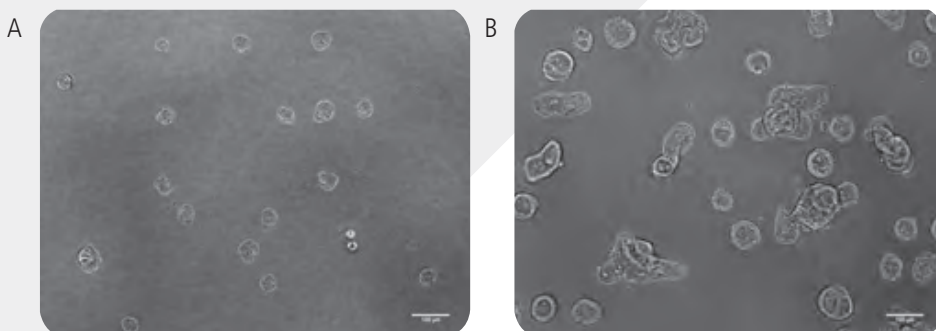
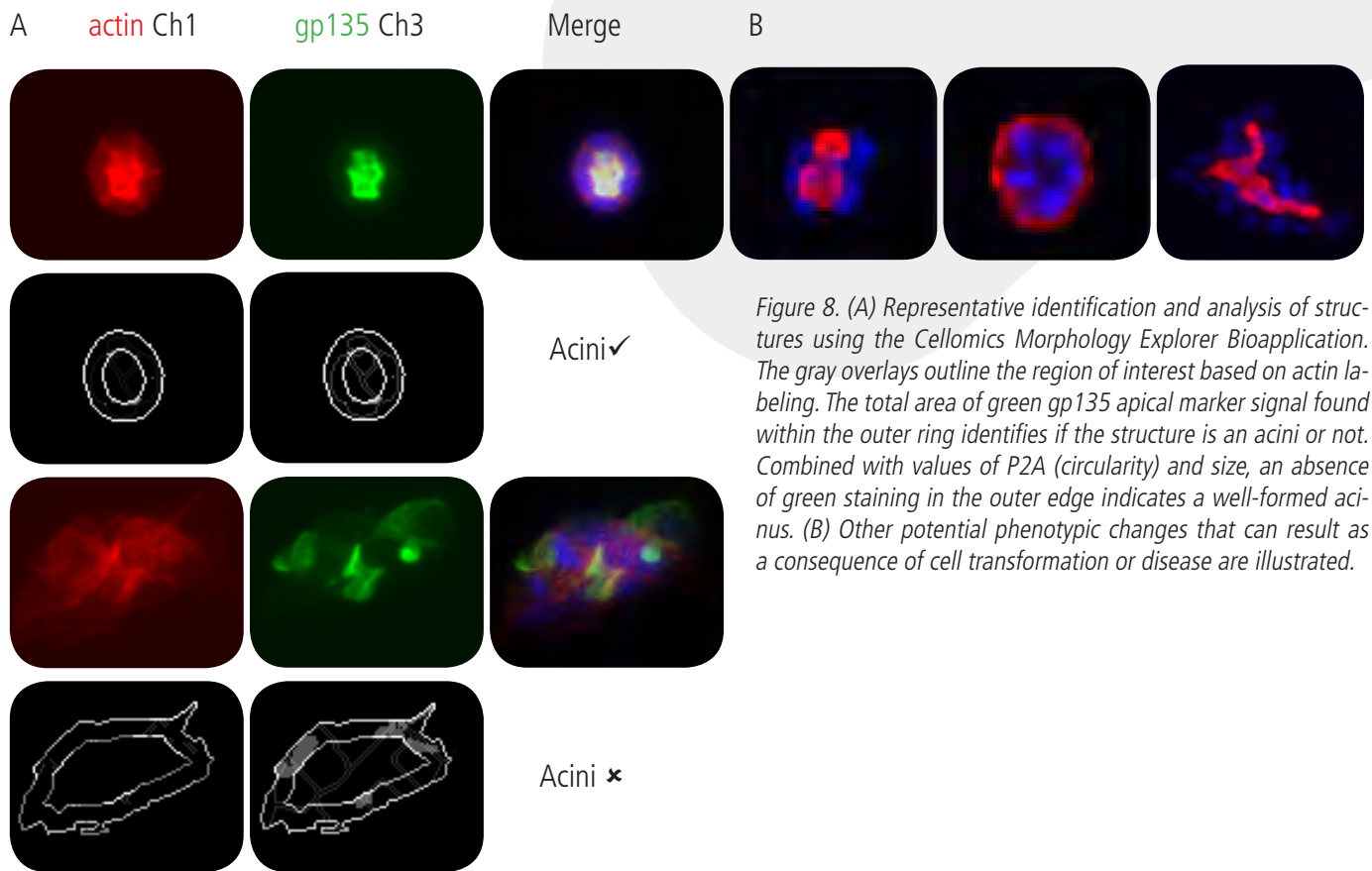


Figure 7. Acini formation in 96-well CYTOOplates. (A) At 3 days, a pitch of 80 μ m between micropatterns is a good compromise between forming individual acini and increasing the number of acini per field of view. (B) At 6 days of acini growth, the 80 μ m pitch is no longer suitable since the acini have grown and begin to fuse into one another and spread. Scale bar: 100 μ m.

📌 Advantages of 2D+ for high-throughput imaging of 3D cultures

In academic labs, scoring of basoapical polarity markers is normally performed by eye. As a result descriptive readouts and quantitative data for polarization are limited to the analysis of a few structures. In this application note, 100-600 structures were scored per sample in each experiment. Samples were imaged on a Cellomics CellInsight Cell Imager using the CYTOOchip or CYTOOplate standard form factor (available through CYTOO or Cellomics). Using just 3 markers, the morphology and polarized status of healthy micropatterned acini can be accurately measured to determine differentiation of epithelial structures. In this example, the apical marker was gp135 detected using antibody from a non-commercial source but this can be replaced by other apically directed proteins such as atypical PKC ζ or prominin for which there are commercial antibodies available. A few features only are enough for acini identification, namely (Cellomics terminology): AreaCh1, ShapeP2ACh1, and SpotFiberTotalAreaCh3 that detects any aberrant signal belonging to the apical marker within the exterior layer of the cyst body. Typical examples of classified Cellomics images are shown in Figure 8A. We found good similarity between human visual inspection and the automated classification calculated by the Cellomics Morphology Explorer Bioapplication with the software identifying polarized acini with 83% accuracy based on the presence or absence of a centralized accumulation of apical protein. These structures can be readily distinguished in screens from disrupted structures that would show multiple cell layers, loss of polarity, hyperproliferation, irregular or enlarged 3D or spread shapes, round spheroids with filled lumens or acini with multilumens (Fig. 8B).



📌 Cyst formation assay development

The CYTOO Acini Array platform can be used as the starting point for 2 types of 3D morphogenesis assays. The first as illustrated above uses maturing acini that can develop over a period of weeks. The second example allows the assay timeframe windows reduced to 24-36h. It is applicable to epithelial cultures such as MDCK cells that preferentially use hollowing to form an apical compartment. With this mechanism, cells become polarized and form a lumen at the 2-cell stage, just after the first cell division¹⁵. This simplified 2-cell 3D culture model overcomes disadvantages associated with imaging thick, light scattering cultures and can be useful for investigating molecular perturbations or engineered mutations that perturb overall acini morphology and cystogenesis. Combined with micropatterns, collagen-I is particularly advantageous for studying early events in lumen formation at the 2-cell stage since MDCK cells growing on collagen-I undergo polarization more slowly and the cells tend to spread out and engage their integrins first. This shorter assay was exploited in the following cited paper and includes the use of drug treatments¹⁶.

📌 Conclusion

The CYTOO Acini Array and 3D MDCK Morphogenesis Assay in chip and 96-well plate formats takes the guesswork out of 3D culture. It can be easily combined with automated imaging and image analysis softwares and bypasses all the problems associated with uneven inconsistent thick gel coating of small 96-wells. Using micropatterns, lumen containing acini are shown here to form on laminin-111, collagen-I and fibronectin coatings and can be scaled up to high throughput format. Such a system now offers the potential to screen and identify novel regulators of epithelial function, differentiation and matrix remodelling. The formation of lumen-containing structures by cells in 3D culture is an established test for cell polarity defects central to certain pathologies and in combination with knock-down or knock-in genetic engineering can be used to model disease states. The results obtained and summarized in Table 3 for MDCKII will not be identical for all 3D cell models since different cell types express different integrin combinations. To date, acini formation on micropatterns has been achieved using other non-transformed lines such as RWPE-1 human prostate cells, human colon cancer-derived Caco-2 cells, LLC-PK1 proximal kidney porcine cells, and NMuMG normal murine mammary cells (Fig. 9).

ECM	Laminin-111		Collagen-I		Fibronectin		
	2D versus 2D+	No pattern	μ pattern	No pattern	μ pattern	No pattern	μ pattern
Lumen formation efficiency (%) at 3 days							
Chip format		70-90	70-90	0	70	0	50
96-well plate		75	60	N.A	40	N.A	N.T
Acini size distribution (CV%)							
Chip format		34	34	N.A	15	N.A	23
Conclusion	Without micropatterns acini collapse and degenerate after 3 days	Laminin coated micropatterns sustain long-term 3D culture. Best conditions for high levels of lumen formation.		N.A	On collagen-I acini formation is dependent on micropatterns. Best conditions for creating a uniform population.	N.A	On fibronectin acini formation is dependent on micropatterns.

Table 3: Performance of conventional 2D flat surfaces compared to 2D+ micropatterns. N.A = Not Applicable. N.T = Not tested

Scientists can thus quickly and conveniently create micropatterned acini cultures with any epithelial immortalized cell line or primary cells that have the capacity to form polarized acini in a three dimensional matrix. To facilitate optimization, CYTOO has designed the **Exploratory Jungle CYTOOplate for Acini Formation** that features a 96 well plate with 20-45 μ m disks spaced at 100-500 μ m intervals in order to choose optimal disk size and pitch during acini formation for assay development with any cell model. CYTOO offers a comprehensive **Exploratory Service & Solutions package** for the development of custom protocols with any cell model on 2D+ micropatterns.

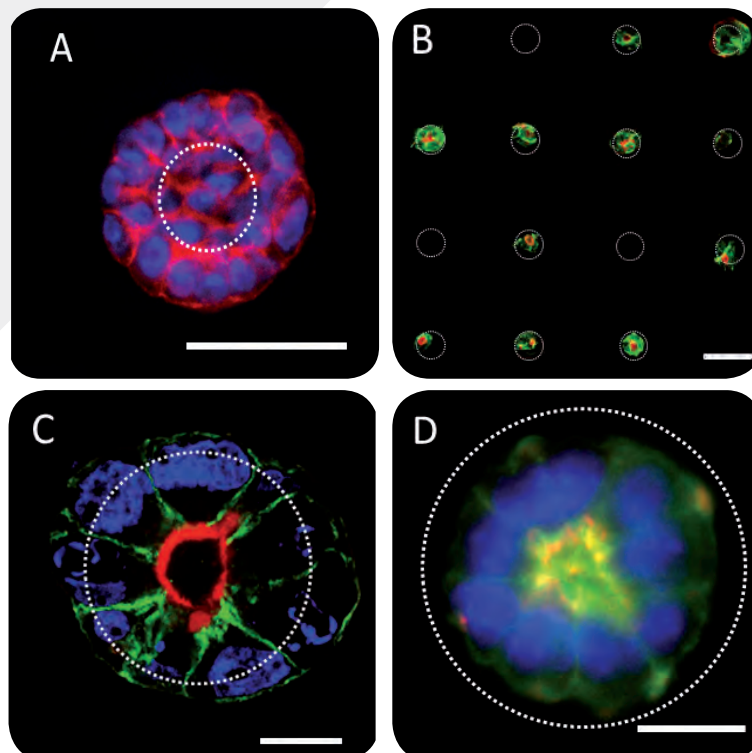


Figure 9: Acini formation by different cell models on 2D+ protein coated micropatterns (A) RWPE-1 prostate acinus at 7 days post seeding on non-coated micropatterns. Scale bar: 50 μ m. (B) LLC-PK-1 acini at 3 days post seeding on laminin coated micropatterns. Scale bar: 50 μ m. (C) Caco-2 acinus at 5 days post seeding on collagen coated micropatterns. Scale bar: 10 μ m. For A) to C) cells are stained to show F-actin (red), B-catenin (green) and nuclei (blue). (D) NMuMG acinus at 7 days post seeding on laminin coated micropatterns. Scale bar: 10 μ m. Cells are stained to show F-actin (green), ZO-1 (red) and nuclei (blue). Micropattern size and position are outlined in white. Images A) and D) are wide field images while B) and C) are confocal. Images are shown with the kind permission of :

A) Monika Dolega and Nathalie Picollet-d'Hahan, CEA Grenoble, iRTSV, France

B) and C) Minerva Bosch and Alejo Rodriguez-Fraticelli from the laboratory of Fernando Martin-Belmonte, CBMSO, Universidad Autonoma de Madrid, Spain.

In the near future, CYTOO's 3D+ portfolio will be expanded to offer additional precision manufactured systems accompanied by standardized cell models and optimized protocols for high throughput production of 3D cell cultures.

Further reading

1. Debnath J, Muthuswamy SK, Brugge JS. Morphogenesis and oncogenesis of MCF-10A mammary epithelial acini grown in three-dimensional basement membrane cultures. *Methods*. 2003;30(3):256–268.
2. Wendt MK, Smith JA, Schiemann WP. Transforming growth factor- β -induced epithelial-mesenchymal transition facilitates epidermal growth factor-dependent breast cancer progression. *Oncogene*. 2010;29(49):6485–6498.
3. Kumar A, Xu J, Brady S, et al. Tissue transglutaminase promotes drug resistance and invasion by inducing mesenchymal transition in mammary epithelial cells. *PLoS ONE*. 2010;5(10):e13390.
4. Sang L, Miller JJ, Corbit KC, et al. Mapping the NPHP-JBTS-MKS protein network reveals ciliopathy disease genes and pathways. *Cell*. 2011;145(4):513–528.
5. Li H, Yang W, Mendes F, Amaral MD, Sheppard DN. Impact of the cystic fibrosis mutation F508del-CFTR on renal cyst formation and growth. *Am. J. Physiol. Renal Physiol*. 2012;303(8):F1176–1186.
6. Qin X-Y, Fukuda T, Yang L, et al. Effects of bisphenol A exposure on the proliferation and senescence of normal human mammary epithelial cells. *Cancer Biol. Ther*. 2012;13(5):296–306.
7. Wang H, Lacoche S, Huang L, Xue B, Muthuswamy SK. Rotational motion during three-dimensional morphogenesis of mammary epithelial acini relates to laminin matrix assembly. *Proc. Natl. Acad. Sci. U.S.A.* 2013;110(1):163–168.
8. Härmä V, Virtanen J, Mäkelä R, et al. A comprehensive panel of three-dimensional models for studies of prostate cancer growth, invasion and drug responses. *PLoS ONE*. 2010;5(5):e10431.
9. Soofi SS, Last JA, Liliensiek SJ, Nealey PF, Murphy CJ. The elastic modulus of Matrigel as determined by atomic force microscopy. *J. Struct. Biol*. 2009;167(3):216–219.
10. O'Brien LE, Jou TS, Pollack AL, et al. Rac1 orientates epithelial apical polarity through effects on basolateral laminin assembly. *Nat. Cell Biol*. 2001;3(9):831–838.
11. Address for gp135 antibody requests: George Ojakian, Professor at Dept of Anatomy and Cell Biology, State University of New York (SUNY) Downstate Medical Center, Brooklyn, NY. george.ojakian@downstate.edu
12. Tseng Q, Duchemin-Pelletier E, Deshiere A, et al. Spatial organization of the extracellular matrix regulates cell-cell junction positioning. *Proc. Natl. Acad. Sci. U.S.A.* 2012;109(5):1506–1511.
13. Engelberg JA, Datta A, Mostov KE, Hunt CA. MDCK cystogenesis driven by cell stabilization within computational analogues. *PLoS Comput. Biol*. 2011;7(4):e1002030.
14. Martín-Belmonte F, Yu W, Rodríguez-Fraticelli AE, et al. Cell-polarity dynamics controls the mechanism of lumen formation in epithelial morphogenesis. *Curr. Biol*. 2008;18(7):507–513.
15. Schlüter MA, Pfarr CS, Pieczynski J, et al. Trafficking of Crumbs3 during cytokinesis is crucial for lumen formation. *Mol. Biol. Cell*. 2009;20(22):4652–4663.
16. Rodríguez-Fraticelli AE, Auzan M, Alonso MA, Bornens M, Martín-Belmonte F. Cell confinement controls centrosome positioning and lumen initiation during epithelial morphogenesis. *J. Cell Biol*. 2012;198(6):1011–1023.

Contact CYTOO for further useful documents:

- Protocol for seeding MDCK cells on CYTOOchips (MO-EXT-19)
- Hints for using Matrigel (MO-EXT-20).



CYTOO Cell Architects

7, parvis Louis Néel - BHT 52, BP50
38040 Grenoble cedex 9 FRANCE
Tel. +33(0) 438 88 47 05

CYTOO, Inc

Harvard Square - One Mifflin Place
Suite 400 Cambridge, MA 02138, USA
Tel. +1 617 674 7711